

Chapter 18

The Use of ^{52}Fe for Bone Marrow Imaging: The Influence of the $^{52}\text{Mn}^m$ Daughter

S. C. Lillicrap

Royal United Hospital, Combe Park, Bath BA1 3NG, U.K.

and

P. H. S. Smith and Heather A. Steere

Physics Department, Royal Marsden Hospital, Sutton, Surrey, U.K.

INTRODUCTION

Iron-59 has been used for a number of years and ^{52}Fe more recently for haematological studies involving the bone marrow and erythropoiesis. The long half-life of ^{59}Fe allows iron incorporation and long-term blood loss to be studied. However, organ imaging with this radionuclide is difficult because of the high-energy gamma emission. The short half-life of the cyclotron-produced positron emitter ^{52}Fe allows much higher activities to be administered and also produces a more clearly resolved image than that obtained with ^{59}Fe . For this reason ^{52}Fe has been used for marrow imaging and short-term plasma clearance studies.

A problem associated with the use of ^{52}Fe in this way is the uncertainty about the fate of the $^{52}\text{Mn}^m$ daughter. A decay scheme showing the major pathways for both ^{52}Fe and $^{52}\text{Mn}^m$ is shown in Fig. 1. Iron-52 decays by electron capture and positron

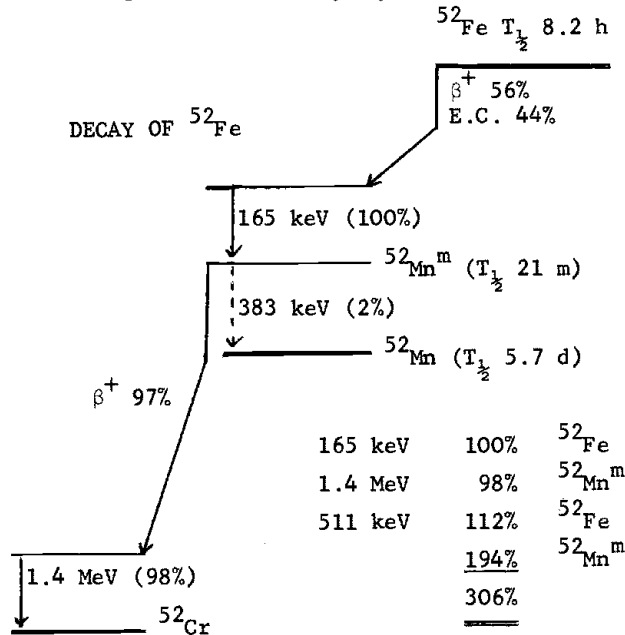


Fig. 1 Major decay pathways for ^{52}Fe and $^{52}\text{Mn}^m$.

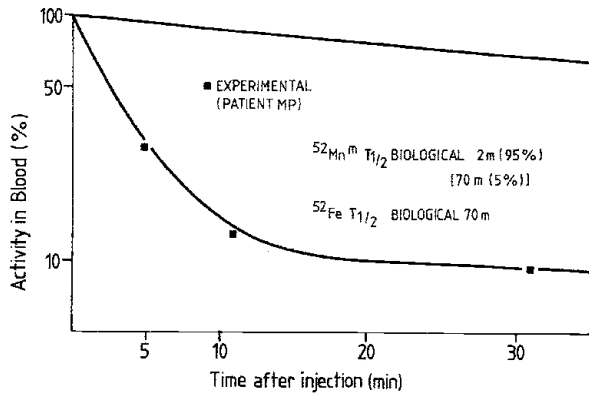


Fig. 2 The clearance of $^{52}\text{Mn}^{\text{m}}$ from the blood of one patient. The squares are the experimental points and the solid line is the calculated fit using the parameters shown. Also shown is the ^{52}Fe clearance from the blood.

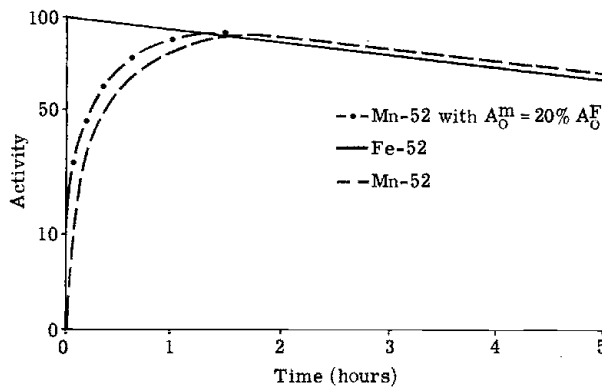


Fig. 3 The kinetics of the $^{52}\text{Mn}^{\text{m}}$ and ^{52}Fe activities in blood immediately after extraction. The curve through the points is the best fit using the parameters shown.

emission into the metastable level of the radioactive daughter ^{52}Mn . Most of the nuclei then decay direct from the metastable level to the 1.4 MeV level of ^{52}Cr . There are therefore three major components to the gamma spectrum: 165 keV photons arising from the ^{52}Fe , 1.4 MeV radiation due to the $^{52}\text{Mn}^{\text{m}}$ and the 511 keV annihilation radiation, one-third from the Fe and two-thirds from the Mn. Therefore when using the 511 keV photons for imaging, as is usual, one is looking predominantly at the distribution of the manganese, not the iron, and it is not possible to distinguish between their distributions. Manganese-52 has a half-life of 21 min, sufficiently long for the possibility that the *in vivo* distribution of the manganese will be different from that of the iron.

The purpose of the present study has been to investigate the kinetics and distribution of the $^{52}\text{Mn}^{\text{m}}$ daughter following intravenous injection of the $^{52}\text{Fe}/^{52}\text{Mn}^{\text{m}}$ mixture for marrow imaging.

RESULTS AND DISCUSSION

On injection, ^{52}Fe contains $^{52}\text{Mn}^{\text{m}}$ in equilibrium. The clearance of $^{52}\text{Mn}^{\text{m}}$ from the blood has been studied on four patients by taking multiple blood samples and measuring the changes in the spectrum as equilibrium is re-established between the ^{52}Fe and the

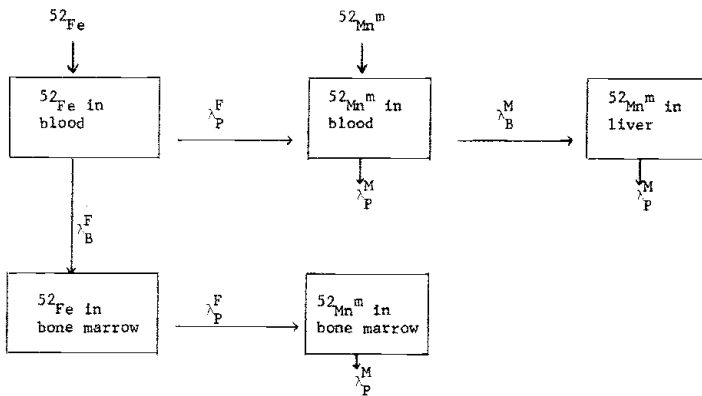


Fig. 4 A simplified compartment model for the kinetics and distribution of ^{52}Fe and $^{52}\text{Mn}^m$ after IV injection.

$^{52}\text{Mn}^m$. All samples were counted in a three-inch well counter. The clearance of $^{52}\text{Mn}^m$ from the blood of one patient is shown in Fig. 2. The squares show the experimental points. The curve which is fitted to the points is discussed later. Also shown is the much slower clearance of the ^{52}Fe from the blood. It can be seen that the initial $^{52}\text{Mn}^m$ is rapidly cleared from the circulation. With the few patients studied the halftime for clearance is in the range 1.5 - 4 min. The clearance of ^{52}Fe from the blood is routinely measured in all patients and for normal persons the halftime is in the range 1 - 2 h. Figure 3 shows the re-establishment of equilibrium between $^{52}\text{Mn}^m$ and ^{52}Fe in the blood sample over the next two hours after extraction.

After separation from the blood it appears that the manganese is taken up by the liver, however a significant proportion may be taken up by other body tissues. This conclusion was first made from the observations of the difference between the scans with ^{52}Fe and those with ^{59}Fe . A survey of 17 patients scanned four hours after receiving ^{52}Fe showed three patients with more than 5% of the activity in the liver, whereas 11 of 17 patients with normal marrow function who received ^{52}Fe showed this amount of liver uptake. At 20 h only 2 of the 17 patients receiving ^{52}Fe had uptake in the liver. The reason for this increased early liver activity following the injection of ^{52}Fe is most probably due to the liver taking up the $^{52}\text{Mn}^m$ circulating in the plasma before the ^{52}Fe is incorporated in the marrow. After 20 h it would appear that the $^{52}\text{Mn}^m$ is bound in the marrow and not reaching the liver.

From these early conclusions it is possible to construct a simplified compartment model as is shown in Fig. 4. In this model the injected ^{52}Fe is taken up by the bone marrow with a halftime of 1 - 2 h. In contrast the injected $^{52}\text{Mn}^m$ is cleared rapidly from the blood with a halftime of 1.5 - 4 min and taken up by the liver. The ^{52}Fe in the blood which decays creates new $^{52}\text{Mn}^m$ and this new manganese is also taken up by the liver. In essence it is a rather complex isotope generator system, with both physical and biological rate constants involved. In this model the lambdas are the rate or transformation constants, the superscript indicating whether it refers to Mn(M) or Fe(F) and the subscript showing whether biological clearance (B) or physical decay (P) is involved.

Using this model the various equations describing the variation of activity with time of the $^{52}\text{Mn}^m$ and ^{52}Fe in the different compartments can be written. The level of the $^{52}\text{Mn}^m$ activity in the blood compartment is described by:

$$A_t^M = \frac{\lambda_P^M}{\lambda_M^M - \lambda_F^F} A_0^F (e^{-\lambda_F^F t} - e^{-\lambda_M^M t}) + A_0^M e^{-\lambda_M^M t}$$

where λ_P^M and λ_F^F are the effective transformation constants, $(\lambda_P^M + \lambda_B^M)$ and $(\lambda_P^F + \lambda_B^F)$ respectively and A_t^M and A_t^F are the activities of the $^{52}\text{Mn}^m$ and ^{52}Fe respectively.

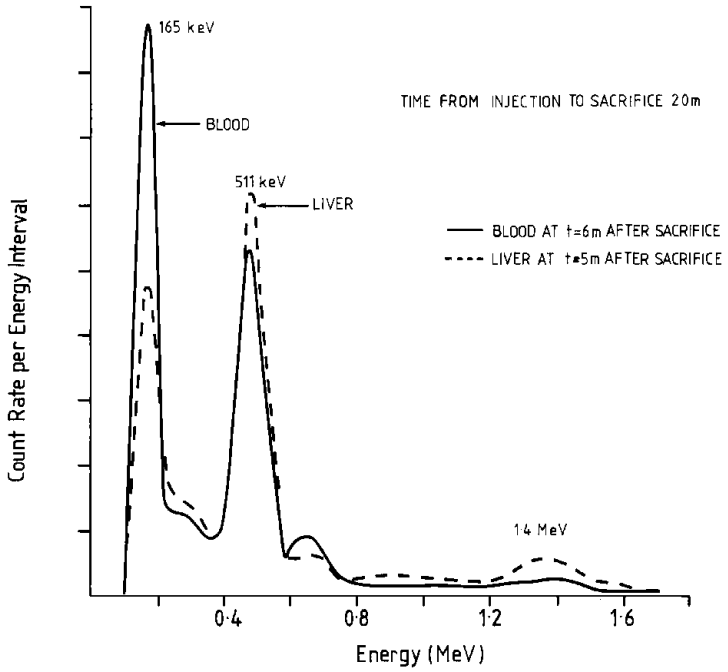


Fig. 5 Spectra of blood and liver of rat shortly after sacrifice.

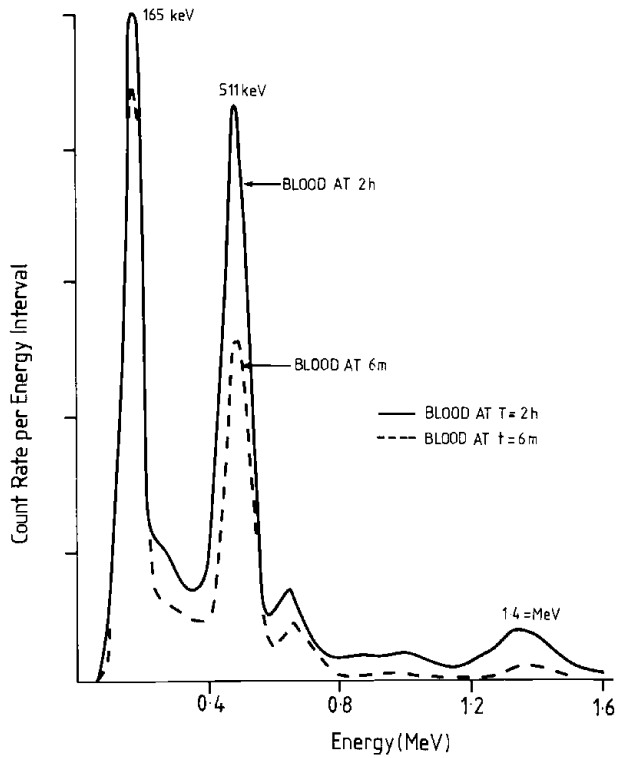


Fig. 6 Spectra of blood of rat 6 min and 2 h after sacrifice.

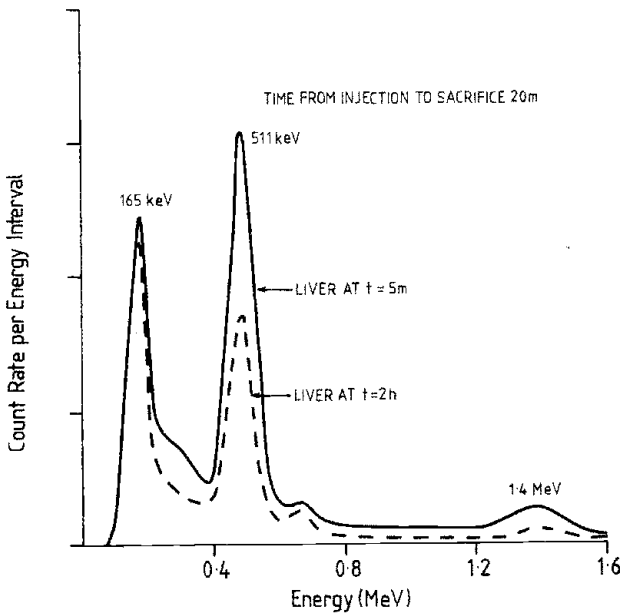


Fig. 7 Spectra of liver of rat 5 min and 2 h after sacrifice.

The line drawn through the manganese points in Fig. 2 is the calculated fit for this patient using a biological halftime for manganese of 2 min (95%) and an iron clearance halftime of 70 min. In order to fit the 30 min point it is assumed that a small proportion (5%) of the manganese remains associated with the iron and is cleared at the same rate.

In addition to the patient observations described earlier further evidence for the fate of the $^{52}\text{Mn}^m$ has been sought from animal experiments. The activity in the blood and liver of rats sacrificed 20 min after injection of ^{52}Fe has been measured and the gamma spectra taken. The differences in the spectra from the blood and the liver samples are illustrated in Fig. 5 which shows the gamma spectra of activity in the blood and the liver of a rat a few minutes after sacrifice. The difference in the spectra is due to a low $^{52}\text{Mn}^m$ content in the blood and a correspondingly high one in the liver. The 165 keV peak is only due to ^{52}Fe and the 1.4 MeV peak only due to $^{52}\text{Mn}^m$. After the blood and liver samples have been removed from the animal, physical equilibrium between the ^{52}Fe and the $^{52}\text{Mn}^m$ is gradually restored as can be seen in Fig. 6 and 7 where, after two hours, the blood and liver spectra have returned to the same 'equilibrium' spectrum. Thus these animal results provide $^{52}\text{Mn}^m$ further evidence that the liver is responsible for the rapid clearance of the $^{52}\text{Mn}^m$ daughter from the blood.

The rapid clearance of the $^{52}\text{Mn}^m$ from the blood, by the liver is of significance in the interpretation of marrow scans when using ^{52}Fe . Using the compartment model in Fig. 4 the $^{52}\text{Mn}^m$ activity in the liver can be calculated in terms of the injected ^{52}Fe activity. Figure 8 shows the calculated variation of the $^{52}\text{Mn}^m$ activity in the liver. After injection, the $^{52}\text{Mn}^m$ activity in the liver will rise to a maximum and then fall with the same halftime as the ^{52}Fe activity in the blood (in this example 100 min). A halftime of 2 min was assumed for the $^{52}\text{Mn}^m$ clearance from the blood. For the $^{52}\text{Mn}^m$ activity in the liver to fall below 10% of the injected ^{52}Fe activity takes at least three biological halftimes which, for a normal patient, is about five hours. Thus if a marrow scan is performed at times shorter than this the scan will generally show liver uptake due to the $^{52}\text{Mn}^m$ activity. If such liver uptake is thought to arise from ^{52}Fe activity an incorrect interpretation of the scan may result.

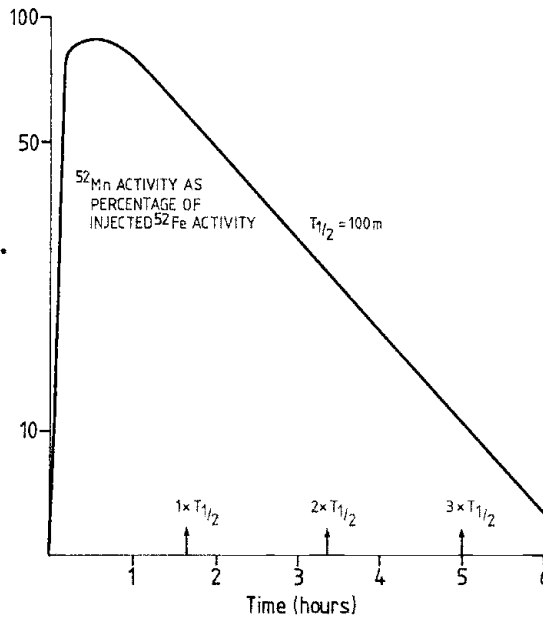


Fig. 8 Calculated variation with time of $^{52}\text{Mn}^m$ activity compared with ^{52}Fe activity.

The above conclusions refer to the $^{52}\text{Mn}^m$ which is rapidly cleared from the blood by the liver. After the parent ^{52}Fe is cleared from the blood and is incorporated in the bone marrow the evidence of the similarity of the ^{52}Fe and $^{52}\text{Mn}^m$ patient scans at 20 h would indicate that at that stage the $^{52}\text{Mn}^m$ daughter is bound in the marrow and not reaching the liver.

CONCLUSIONS

These investigations on the fate of the $^{52}\text{Mn}^m$ daughter would indicate that when ^{52}Fe is used for erythropoietic marrow imaging care must be taken in the interpretation of the scans performed within the first few hours of injection, but that thereafter they may be taken to represent the true iron distribution.

REFERENCE

1. D.C. Borg and G.C. Cotzias, *J. Clin. Invest.* 37, 1269 (1958).

ACKNOWLEDGEMENTS

The authors would like to thank Dr David Taylor, head of Department of Radiopharmacology for his generous collaboration in the animal experiments and Mr P. Moden for his most helpful assistance.

DISCUSSION

L. BURKINSHAW: Was the smooth curve in your final slide a theoretical recovery curve, or was it derived from the data?

S.C. LILICRAP: No, it was not a theoretical recovery curve. It was a crude mean curve drawn through the experimental points. The data did not justify more sophisticated curve-fitting.